This article has been accepted for publication in a future issue of this journal, but has not been fully edited. Content may change prior to final publication. Citation information: DOI 10.1109/LPT.2017.2723606, IEEE Photonics Technology Letters

Subtraction-Clustering-Based Modulation Format Identification in Stokes Space

Pengyu Chen, Jie Liu, Xiong Wu, Kangping Zhong, and Xiaofeng Mai

***Abstract*—A Stokes-space-based modulation format identification (MFI) technique with low complexity is proposed for coherent optical receivers, on the basis of the subtraction clustering algorithm. Successful MFI with good OSNR performance can be realized among polarization-multiplexed BPSK, QPSK, 8PSK, 8QAM and 16QAM signals. Experimental verifications are also performed to prove the feasibility of the proposed MFI in long-distance optical fiber transmission systems.**

***Index Terms*—Coherent detection, modulation format identification (MFI), polarization multiplexing, optical fiber communication, Stokes space, subtraction clustering.**

I. Introduction

COGNITIVE optical networks (CONs) combined with the techniques of coherent detection and digital signal processing (DSP), providing flexible bandwidth allocation and high spectral efficiency, have been considered a promising solution for next generation optical networks [1]. In CONs, adaptive transmission parameters, such as modulation format, data rate, etc., are required at the transmitters of CONs, to accommodate the dynamic traffic requirements as well as increase the spectral efficiency [2]. As a result, it is necessary for the receivers in CONs to blindly retrieve these transmission parameters from the received signals, so that proper activities can be adopted subsequently to achieve the optimum performance. In particular, modulation format identification (MFI) becomes essential for the receivers in CONs.

MFI techniques have entensively developed in wireless communication domain [3]. By contrast, MFI techniques in the field of optical fiber communication are still at the early stage with great potential for research. Several MFI approaches have been proposed in previous literatures for the optical fiber communication systems [4]-[8]. Among these techniques, the Stokes-space-based MFI techniques are quite attractive, as they are independent of the carrier phase noise, frequency offset and polarization mixing [6]-[8]. However, most of Stokes-space-based MFI schemes proposed by now require machine learning algorithms with high complexity, such as expectation maximization algorithm [6], [7], maximum likelihood algorithm [8], etc.

In this paper, a blind MFI technique with low complexity is proposed for the coherent optical receivers, on the basis of subtraction clustering algorithm combined with a hybrid analysis method. Successful MFI among modulation formats of BPSK, QPSK, 8PSK, 8QAM and 16QAM can be realized in the dual-polarization simulation system within practical optical signal-to-noise ratio (OSNR) range. Comparisons between the proposed MFI technique and other clustering-algorithm-based MFI schemes in Stokes space are also performed, showing that good optical OSNR performance but lower complexity can be achieved by utilizing our method. In addition, experiment demonstrations of polarization multiplexed (PM)-QPSK and PM-16QAM systems are also implemented to verify the proposed MFI technique in long-distance fiber-optic transmission systems..

II. Operating Principles and Simulation Results

The DSP module with MFI capability for coherent optical communication system is shown in Fig. 1. The proposed MFI algorithm is placed after the modulation format-independent algorithms [timing phase recovery and chromatic dispersion (CD) compensation] [9], [10] and before the modulation format-dependent algorithms (adaptive equalization for polarization demultiplexing, frequency offset compensation and carrier phase estimation) [11]. The proposed MFI scheme

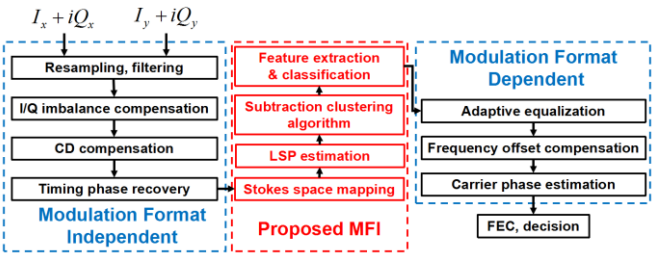

Fig. 1. DSP module with proposed MFI method for coherent optical communication system.

mainly includes three steps: Stokes space mapping and least square plane (LSP) estimation, subtraction clustering as well as feature extraction and classification. Details will be presented in the following parts of this section.

Manuscript received April 14, 2017; revised May 10, 2017; accepted June 27, 2017. This work was supported by Natural Science Foundation of China under grant No. 61505266 and Natural Science Foundation of Guangdong province, China under grant No. 2014A030310364 and grant No. 2016A030313289.

P. Chen and X. Mai are with the State Key Laboratory of Optoelectronic Materials and Technologies, School of Electronics and Information Technology, Sun Yat-sen University, and they are also with School of Data and Computer Science, Sun Yat-sen University, Guangzhou 510006, China.

J. Liu, and X. Wu are with the State Key Laboratory of Optoelectronic Materials and Technologies, School of Electronics and Information Technology, Sun Yat-sen University, Guangzhou 510006, China (e-mail: liujie47@mail.sysu.edu.cn).

K. Zhong is with the Photonics Research Centre, Department of Electronics and Information Engineering, The Hong Kong Polytechnic University, Hung Hom, Kowloon, Hong Kong

1041-1135 (c) 2017 IEEE. Personal use is permitted, but republication/redistribution requires IEEE permission. See http://www.ieee.org/publications_standards/publications/rights/index.html for more information.

This article has been accepted for publication in a future issue of this journal, but has not been fully edited. Content may change prior to final publication. Citation information: DOI 10.1109/LPT.2017.2723606, IEEE Photonics Technology Letters

A. Stokes Space Mapping and LSP estimation

Assuming e_x and e_y are the two received signals with polarization multiplexing, which are timing phase recovered, chromatic dispersion (CD) compensated and power normalized, they can be mapped to the Stokes space by using the following equations [12]:

$$S=\begin{bmatrix}S_0\\S_1\\S_2\\S_3\end{bmatrix}=\frac{1}{2}\begin{bmatrix}e_xe_x^*+e_ye_y^*\\e_xe_x^*-e_ye_y^*\\e_xe_y^*+e_ye_x^*\\je_xe_y^*-je_ye_x^*\end{bmatrix}=\frac{1}{2}\begin{bmatrix}a_x^2+a_y^2\\a_x^2-a_y^2\\2a_xa_y\cos\Delta\phi\\2a_xa_y\sin\Delta\phi\end{bmatrix} \quad (1)$$

where a_x and a_y are the amplitude of e_x and e_y, respectively. And $\Delta\phi$ denotes the phase difference between e_x and e_y, which is independent of polarization rotation. The vector $(S_1, S_2, S_3)^{\mathrm{T}}$ represents the three dimensions Stokes space constellations. The constellation of PM signals in Stokes space is proved to be a lens-like object, and the symmetric plane of the lens-like object, which is called LSP, can be obtained by least square fitting based on Singular Value Decomposition (SVD) [12]. Here we note that when there is no polarization rotation, the LSP coincides with the S_2-S_3 plane, while the normal plane of the LSP coincides with the S_1-S_3 plane.

B. Subtraction Clustering Algorithm

We consider there are totally N data points. After mapped to the Stokes space, the density index of the k_{th} data point on the LSP or the normal plane of the LSP can be designed as [13]:

$$D_k=\sum_{j=1}^{N}\exp\left(-\frac{\|r_k-r_j\|^2}{K_a\gamma_a^2}\right) \quad (2)$$

where $\|r_k-r_j\|$ means the Euclidean distance between the k_{th} data point and one of all other data points. K_a is the adjustment coefficient whose value is set to 1/11 here. γ_a denotes the density contributed radius, data points outside which have little influence on the density index. γ_a can be calculated as:

$$\gamma_a{}^2=\frac{1}{N}\sum_{k=1}^{N}|p_k|^2 \quad (3)$$

where $|p_{\mathrm{k}}|$ is the absolute value of the k_{th} data point. After calculation of the density index of each point, the point with the largest density index is chosen as the first cluster center, and then the density index of the other points is updated as following equation:

$$D_k=D_k-D_1^*\exp\left(-\frac{\|r_k-r_1^*\|^2}{K_b\gamma_a^2}\right) \quad (4)$$

where r_1^* represents the location of the first cluster center with density index D_1^*. By subtracting an amount of density index as a function of the distance from the first cluster center, the data points near the first cluster center will have greatly reduced density index. K_b is the coefficient utilized to adjust density decreased index, whose value is set to 1.5 /11 (equals to $1.5K_a$) to avoid the new cluster center too close to the first one [13]. After revising the density index of all the data points except the first cluster center according to Equation (4), the data point with the highest newly updated density index is selected as the new potential cluster center and sent to the next accepting/rejecting-cluster-center scenario (details will be presented in the next paragraph). If the result of the accepting/rejecting-cluster-center scenario is positive, the density index of the left data points can be updated according to their distance to the second cluster center. After the m_{th} cluster center has been found, density index of each point can be updated by the following equation:

$$D_k=D_k-D_m^*\exp\left(-\frac{\|r_k-r_m^*\|^2}{K_b\gamma_a^2}\right) \quad (5)$$

where r_m^* represents the location of the m_{th} cluster center with density index D_m^*.

The accepting/rejecting-cluster-center scenario can be according to the following criteria: (1) If density ratio R_{k} of the k_{th} selected potential cluster center, which can be calculated as $R_{\mathrm{k}}=D_{\mathrm{k}}/D_{\max}$, is no less than the accepting ratio R_{ac}, this potential cluster center will be considered as a new cluster center; (2) if R_{k} is no more than the rejecting ratio R_{re}, the potential cluster center under test will be removed and the clustering process will be ended; (3) if $R_{\mathrm{re}}<R_{\mathrm{k}}<R_{\mathrm{ac}}$, a new decision procedure is required to consider whether the potential cluster center under test is a new cluster center or not. Details of the decision procedure are: if $R_{\mathrm{k}}+d_{\min}/\gamma_a\geq 1$, where $d_{\min}$ denotes the shortest distances between the potential cluster center under test and all previously found cluster centers, this potential cluster center will be accepted as a new cluster center, or D_{k} will be set to 0 and select the point with next highest density index and follow the criteria above.

Note that we set R_{ac}=0.5 and R_{re}=0.15 for identification of all the five modulation formats. After the subtraction clustering, the cluster centers with distance between each other smaller than a certain value 0.33 will be attributed to one cluster center with the location of their mean value.

C. Feature Extraction, Classification and Simulation Results

After subtraction clustering, constellations on the LSP and its normal plane can be represented by the extracted cluster centers, as shown in Fig. 2. This means that signals with different modulation formats can be identified based on the statistical parameters of the cluster centers distributed on the LSP and its normal plane. The decision flow chart is shown in Fig. 3 and the decision metrics of different kinds of modulation formats are depicted in Fig. 4. Here N_{23} and N_{13} denote the number of clusters centers distributed on the LSP and its normal plane, respectively. $C_{4,1}$ and $C_{4,0}$ are high-order cumulants of cluster centers of LSP, which can be calculated as the following equation [14]:

$$C_{4,0}=\frac{1}{n}\sum_{k=1}^{n}y_k^4-3\left(\frac{1}{n}\sum_{k=1}^{n}y_k^2\right)^2,\quad C_{4,1}=\frac{1}{n}\sum_{k=1}^{n}y_k^3y_k^*-3\frac{1}{n}\sum_{k=1}^{n}y_k^2\frac{1}{n}\sum_{k=1}^{n}|y_k|^2 \quad (6)$$

where y_{k} denotes the k_{th} cluster point after subtraction algorithm, and ID_{pq} is defined as following equation:

$$ID_{\mathrm{pq}}=a\ \mathrm{var}_{\mathrm{n}}+b\ \mathrm{var}_{\mathrm{dis}} \quad (7)$$

where $\mathrm{var}_{\mathrm{n}}$ and $\mathrm{var}_{\mathrm{dis}}$ are the variance of modulus of cluster centers distributed on normal direction of LSP and LSP, respectively. a and b are weight coefficients and we set a = 0.2

1041-1135 (c) 2017 IEEE. Personal use is permitted, but republication/redistribution requires IEEE permission. See http://www.ieee.org/publications_standards/publications/rights/index.html for more information.

This article has been accepted for publication in a future issue of this journal, but has not been fully edited. Content may change prior to final publication. Citation information: DOI 10.1109/LPT.2017.2723606, IEEE Photonics Technology Letters

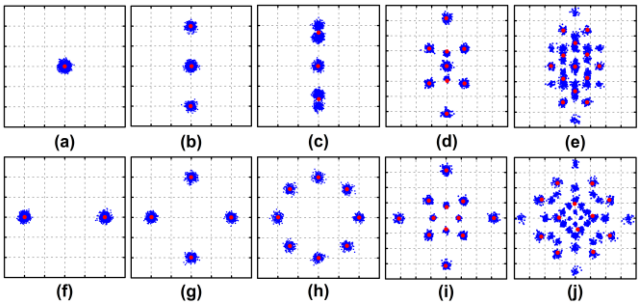

Fig. 2. Clustering results of the PM signals on the normal plane of the LSP (a)-(e), and on the LSP (f)-(j) at relatively high OSNRs. Columns from left to right are BPSK, QPSK, 8PSK, 8QAM and 16QAM, respectively. The red points mean the cluster centers.

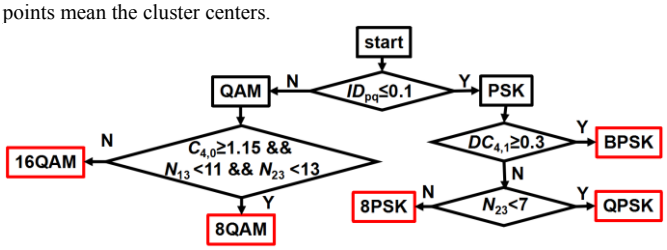

Fig. 3. Flow chart of the MFI processing block and decision tree.

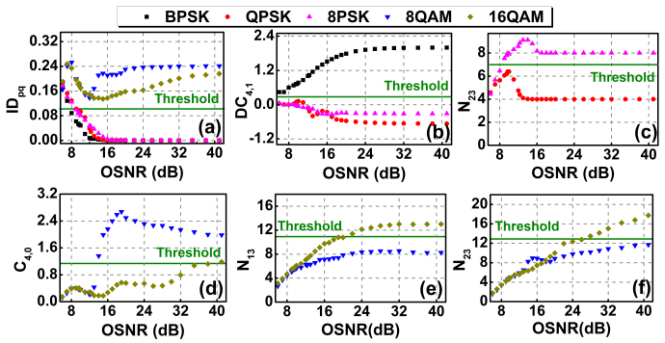

Fig. 4. Simulation results of decision metrics versus OSNR.

and b = 0.8. $DC_{4,1}$ is used to identify BPSK which represents the difference of $C_{4,1}$ of LSP and normal plane of LSP.

Dual-polarization simulation system with 28GBaud signals transmitting through an additive Gaussian white noise channel was implemented by using MATLAB to evaluate the performance of the proposed MFI technique. In the simulation system, a fourth-order low-pass Bessel filter with bandwidth of 20 GHz was utilized to simulate the bandwidth-limited transceiver. And the effective number of bits (ENOB) of the analog-to-digital convertor (ADC) or DAC at the transceivers was set to 8 bits. Before the MFI algorithm, conventional DSP algorithms such as resampling and filtering, CD compensation [9] and timing phase recovery [10] were utilized to give a signal pre-processing. Fig. 5 shows the simulation results. Here note that 100 independent simulations were conducted for each OSNR and 2000 samples were utilized in each run. It can be seen from the simulation results that virtually 100% correct identification of the five modulation formats is achieved for OSNRs greater or equal to their respective forward error correction (FEC) thresholds. Particularly, identification of 16QAM signal achieves the best OSNR performance among those of the five modulation formats. If high-order QAM signals, such as 32QAM or 64QAM signals, are considered, the OSNR performance of the identification of QAM signals might

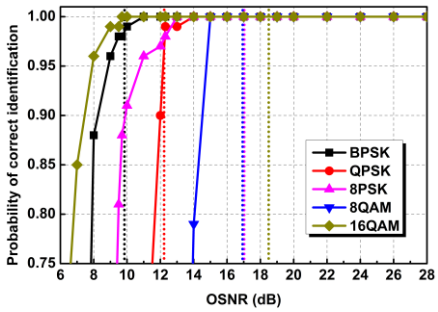

Fig. 5. Simulation results of classification performances versus OSNR. The dot lines (same color with the corresponding data curves) represent OSNR thresholds corresponding to FEC correcting BER of 3.8e-3 of the corresponding modulation formats.

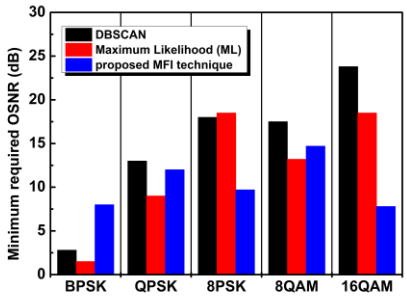

Fig. 6. Test of OSNR performances(minimum required OSNR to achieve reliability higher than 95%).

be deteriorated. Some powerful machine learning algorithms, such as support vector machines, could improve the identification performance when high-order QAM signals are considered [15]. However, complexity will be another factor to consider in this case. There should be a tradeoff between complexity and performances of the MFI algorithm in practical implementations.

Performance comparisons were also implemented between the proposed MFI technique and clustering-algorithm-based MFI schemes in Stokes space in previous literature [8]. According to the analysis in [8], the density-based spatial clustering of applications with noise (DBSCAN) has relatively lower complexity, and Maximum-likelihood (ML) based algorithm has relative better OSNR performance. As a result, they were chosen for comparison, and simulation results are shown in Fig. 6. As for the MFI algorithms based on subtraction clustering and DBSCAN, the algorithm complexity is mainly attributed to the clustering algorithm, since no complex or iterative calculation in the process of Stokes space mapping, as well as feature extraction and classification. The complexity of DBSCAN is O(n*log$_2n$) when spatial access method is utilized [16], while complexity of subtraction clustering algorithm is O(n*m) [13]. As for the ML algorithm, it made use of Silhouette coefficients [8], which contributed the complexity of around O(n^2). Here note that n and m refers to the number of symbols under test and iterations, respectively. In our simulation, 2000 symbols were utilized for test and the average iteration times of the subtraction clustering algorithm are around 30. As a result, the complexity of our proposed MFI algorithm is quite similar with that of DBSCAN, but much lower than that of the ML algorithm theoretically. In addition, better or similar OSNR performance can be achieved by using

1041-1135 (c) 2017 IEEE. Personal use is permitted, but republication/redistribution requires IEEE permission. See http://www.ieee.org/publications_standards/publications/rights/index.html for more information.

This article has been accepted for publication in a future issue of this journal, but has not been fully edited. Content may change prior to final publication. Citation information: DOI 10.1109/LPT.2017.2723606, IEEE Photonics Technology Letters

the proposed MFI technique for high order modulation formats from QPSK to 16QAM, compared with other two MFI algorithms.

III. Experiment Verification

Proof-of-concept experiment was also implemented to prove the feasibility of the proposed MFI scheme. The experiment setup is shown in Fig. 7. At the transmitter, by using an optical I/Q modulator, optical light from an external cavity laser (ECL) was modulated by 28GBaud QPSK and 16QAM electrical signals, which are generated from an arbitrary waveform generator (AWG). Then the generated optical signals were split into two branches by a polarization beam splitter (PBS), decorrelated by an optical delay line and combined by a polarization beam combiner (PBC) to generate PM optical signals. After amplified by an Erbium doped fiber amplifier (EDFA), the PM signals were launched to an optical fiber

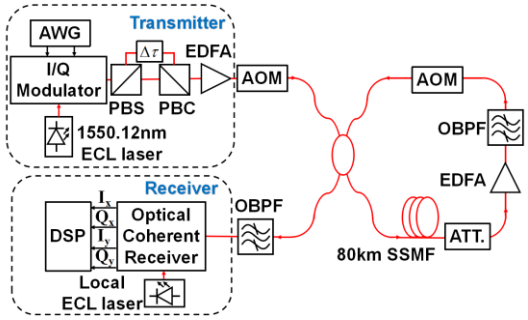

Fig. 7. Experimental setup.

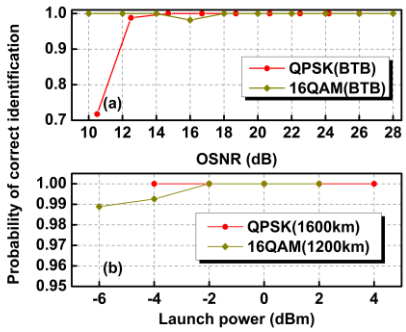

Fig. 8. Experimental results of classification performances for 28Gbaud QPSK and 16QAM signals: (a) in the back-to-back (BTB) configuration; (b) after long distance transmission at different launch powers.

recirculating loop with 80-km standard single mode fiber (SSMF) span. Finally the optical signals were detected by a coherent optical receiver, sampled by an real-time oscilloscope for off-line DSP.

The measured probabilities of correct identification at different OSNRs (BTB) or optical power launched to the fiber (after fiber transmission) are depicted in Fig. 8. In the measurement, average of 250 discontinuous data sequence with 2000 test symbols in each sequence were captured for each OSNR or optical power launched to the fiber. As the BTB results shown in Fig. 8, similar OSNR performance can be achieved compared with simulation results shown in Fig. 5 for both of the two signals. With respect to the results after fiber transmission, nearly 100% correct identification can be realized for both of the PM-QPSK and PM-16QAM signals within practical optical power ranges launched to the fiber, indicating the proposed MFI technique is resilient towards fiber impairments.

IV. Summary

We have proposed a Stokes space MFI technique based on the subtraction clustering algorithm for digital coherent optical receivers. Successful MFC among PM-BPSK, PM-QPSK, PM-8PSK, PM-8QAM, and PM-16QAM signals has been demonstrated in numerical simulations. Performance comparisons between the proposed MFI algorithm and other clustering-algorithm-based MFI schemes in Stokes space show that good OSNR performance can be achieved for the proposed MFI scheme but with low complexity. Experimental demonstration in PM-QPSK and PM-16QAM systems have also been implemented to prove the feasibility of the proposed MFI technique in the practical long-distance fiber optic systems.

References

[1] W. Wei, C. Wang, and J. Yu, "Cognitive optical networks: Key drivers, enabling techniques, and adaptive bandwidth services" *IEEE Commun. Mag.*, vol. 50, no.1, pp. 106-113, Jan. 2012.

[2] K. Roberts and C. Laperle, "Flexible transceivers," in European Conference and Exhibition on Optical Communication, OSA Technical Digest (online) (Optical Society of America, 2012), paper We.3.A.3.

[3] O. A. Dobre, A. Abdi, Y. Bar-Ness and W. Su, "Survey of automatic modulation classification techniques: classical approaches and new trends" *IET Commun.*, vol.1, no.2, pp. 137-156, Apr. 2007.

[4] F. N. Khan, Y. Zhou, A. P. T. Lau, and C. Lu, "Modulation format identification in heterogeneous fiber-optic networks using artificial neural networks," *Opt. Express*, vol.20, no.11, pp. 12422-12431, 2012.

[5] J. Liu, Z. Dong, K. P. Zhong, et al, "Modulation format identification based on received signal power distributions for digital coherent receivers," in Optical Fiber Communication Conference, OSA Technical Digest (online) (Optical Society of America, 2014), paper Th4D.3.

[6] R. Borkowski, D. Zibar, A. Caballero, V. Arlunno, and I. T. Monroy, "Stokes space-based optical modulation format recognition for digital coherent receivers," *IEEE Photon. Technol. Lett.*, vol. 25, no. 21, pp. 2129-2132, Nov.1, 2013.

[7] P. Isautier, J. Pan, R. DeSalvo, and S. E. Ralph, "Stokes space-based modulation format recognition for autonomous optical receivers," *J. Lightw. Technol.*, vol.33, no.24, pp. 5157-5163, Dec.15, 2015.

[8] R. Boada, R. Borkowski, and I. T. Monroy, "Clustering algorithms for Stokes space modulation format recognition," *Opt. Express*, vol. 23, no.12, pp. 15521-15531, 2015.

[9] R. Kudo, T. Kobayashi, K. Ishihara, Y. Takatori, A. Sano, and Y. Miyamoto, "Coherent optical single carrier transmission using overlap frequency domain equalization for long-haul optical systems," *J. Lightw. Technol.*, vol.27, no.16, pp.3721-3728, Aug.15, 2009.

[10] D. Godard, "Pass band timing recovery in an all-digital modem receiver," *IEEE Trans. Commun.*, vol.26, no.5, pp. 517-523, May. 1978.

[11] E. Ip, A. P. T. Lau, D. J. Barros, and J. M. Kahn, "Coherent detection in optical fiber systems," *Opt. Express.*,vol. 16, no. 2, pp. 753–791, 2008.

[12] B. Szafraniec, B. Nebendahl, and T. Marshall, "Polarization demultiplexing in Stokes space,"*Opt. Express*, vol.18, no.17, pp. 17928-17939 , 2010.

[13] S. Chiu, "Fuzzy model identification based on cluster estimation," *J. of Intelligent & Fuzzy Systems*, vol. 2, no. 3, 1994.

[14] A. Swami and B. M. Sadler, "Hierarchical digital modulation classification using cumulants," *IEEE Trans. Commun.*, vol. 48, no. 3, pp. 416-429, Mar. 2000.

[15] J. Thrane *et al.*, "Machine learning techniques for optical performance monitoring from directly detected PDM-QAM signals," *J. Lightw. Technol.,* vol.35, no.4, pp.868-875, Feb. 15, 2017.

[16] M. Ester, H. P. Kriegel, J. Sander, and X. Xu, "A density-based algorithm for discovering clusters in large spatial databases with noise," in Second International Conference on Knowledge Discovery and Data Mining, pp. 226 – 231, 1996.

1041-1135 (c) 2017 IEEE. Personal use is permitted, but republication/redistribution requires IEEE permission. See http://www.ieee.org/publications_standards/publications/rights/index.html for more information.